Supporting Information for:

Exploring Chemistry in Microcompartments Using Guided Droplet Collisions in a Branched Quadrupole Trap Coupled to a Single Droplet, Paper Spray Mass Spectrometer

Michael I. Jacobs,[1,2] James F. Davies,[2] Lance Lee,[2,†] Ryan D. Davis,[2] Frances Houle,[2] Kevin R. Wilson[2,*]

[1]Department of Chemistry, University of California, Berkeley, CA 94720, United States

[2]Chemical Sciences Division, Lawrence Berkeley National Laboratory, Berkeley, CA 94720, United States

[†]Now at Stanford Linear Accelerator Center, Menlo Park, CA 94025

* Correspondence to: krwilson@lbl.gov, (510) 495-2474

Table of Contents:

S1. Measuring kinetics in bulk:

Equal amounts (1 mL) of the same OPA and alanine solutions used in droplet experiments are mixed and vigorously stirred in a quartz cuvette. The 355 nm laser (attenuated with a neutral density filter) is directed into the cuvette and fluorescence is imaged at 90° after filtering with a bandpass filter (450±20 nm) using a CCD camera (Thorlabs). Images are collected at 10 Hz with a 30 ms exposure. Because fluorescence intensity decreases across the path length of the cuvette (due to strong absorption of the 355 nm light by the fluorescent product), fluorescence intensity at the front of the cuvette (where the laser enters) is tracked over the course of the reaction. An image exposure is chosen such that this intensity scales linearly with concentration of expected fluorescent product. Reactions in the cuvette are monitored for ~100 s, and each reaction condition is run in triplicate.

S2. Measuring relative speeds of merging droplets:

The effect of the balancing electrode on the velocity of the merging electrode is investigated by imaging droplets in the near field as they approach the electrode. Typical merging droplet conditions are applied (i.e. the voltage applied to the induction electrode is set such that falling droplets would be attracted to both a held droplet and the balancing electrode), and droplets are dispensed at 100 Hz without a held droplet in the trap. The droplets are illuminated using the 532 nm laser and imaged with a CMOS camera (Thorlabs, Inc.) with a 1 ms exposure. The velocity of the droplets visually increases when the voltage applied to the balancing electrode increases. The length of a droplet streak in the images collected by the camera is used to determine how the velocity of the falling droplet changes as larger voltages are applied. As shown in Figure S-3, the length of the streak (and velocity of the droplet) increases by 30 and 60% (compared to free fall) when 250 and 500 V are applied to the balancing electrode, respectively. Experiments typically apply ~100 V to the balancing electrode to hold a droplet before merging. Thus, the speed of the merging droplet is not expected to increase considerably (~10%) due to the attraction toward the balancing electrode. Additionally, the charge on the droplet (~10^{-13} C) is not large enough to affect the speed of collision. Thus, the terminal velocity of the merging droplet is a good measure of the speed of collision in the experiments reported here.

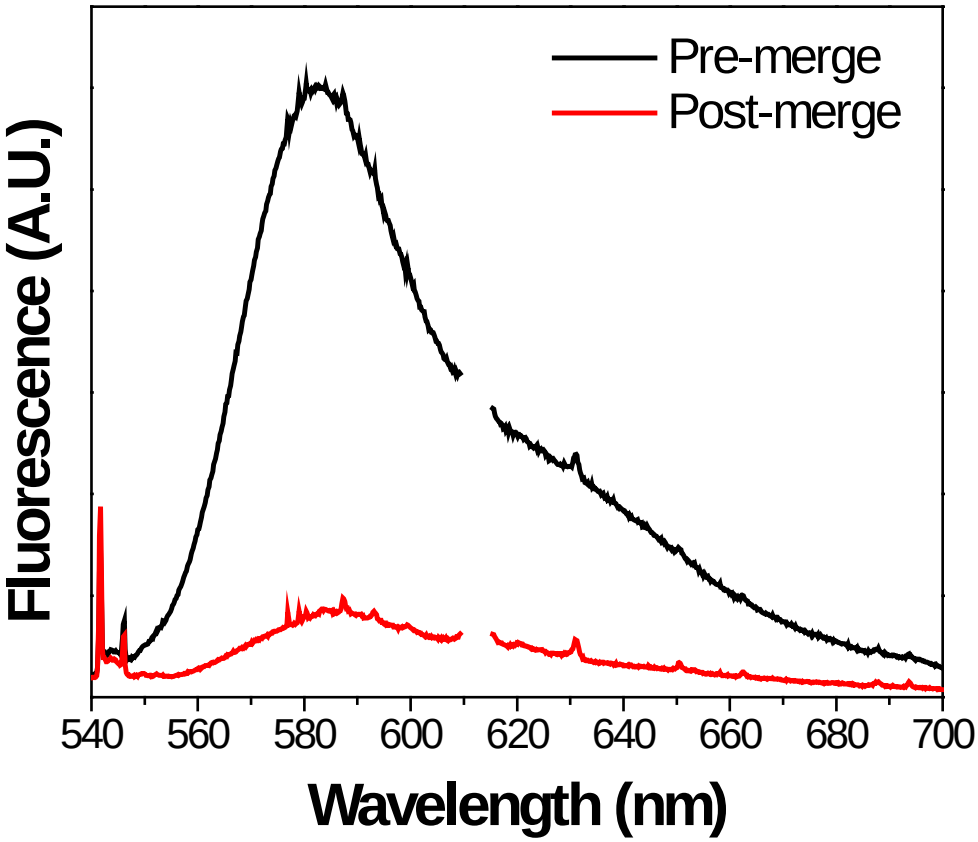

Figure S-1. Fluorescence spectra of trapped droplets containing 500 μM RhB before and after merging with a 20% (v/v) sulfuric acid droplet. The fluorescence intensity drops considerably with the decrease in pH. Fluorescence spectra from the droplets are collected using an Ocean Optics QE Pro-Raman spectrometer.

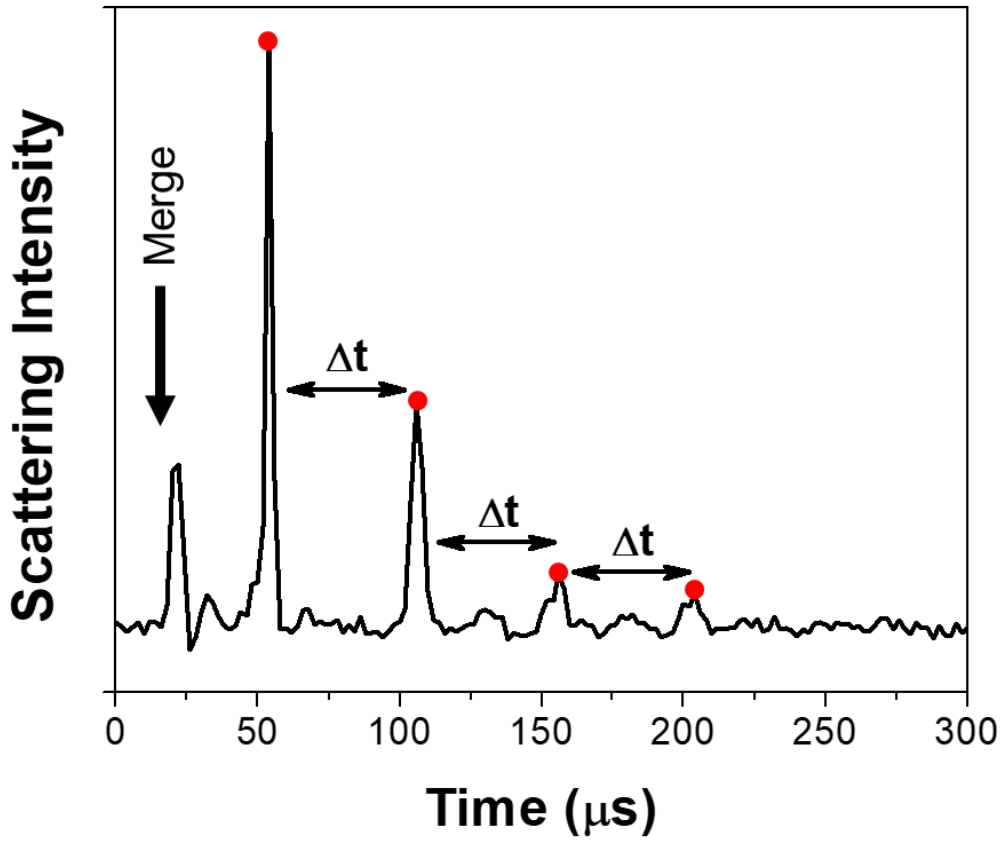

Figure S-2. Elastically scattered light intensity as a result of ~3 M LiCl droplet coalescence (measured at 90°). A droplet with a radius of 23.0±0.6 µm coalesces with a droplet with radius of 25.2±0.2 µm to yield a merged droplet with a radius of 30.4±0.4 µm. The black arrow shows the point in time when the droplets merge together. As the initially dumbbell shaped droplet relaxes back to spherically shaped, resonances in scatter intensity are observed. The angular frequency of these resonances and the decay of their intensity can be used to calculate surface tension and viscosity of the merged droplet, respectively.

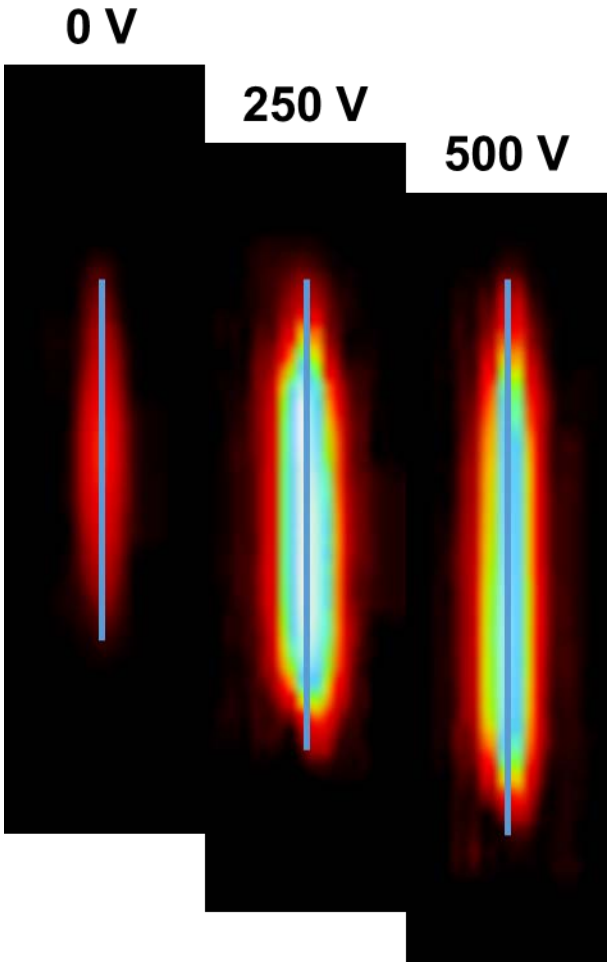

Figure S-3. Droplets imaged with a 1 ms exposure as they approach the balancing electrode set to different potentials (0, 250 and 500 V). As the potential on the electrode increases, the Coulombic attraction is greater and the droplet travels faster, leading to longer streaks. Based on the lengths of the streaks, the velocity of the droplets approaching the balancing electrode with 250 and 500 V applied are 30% and 60% faster than droplets falling at terminal velocity (i.e. no potential applied to balancing electrode).

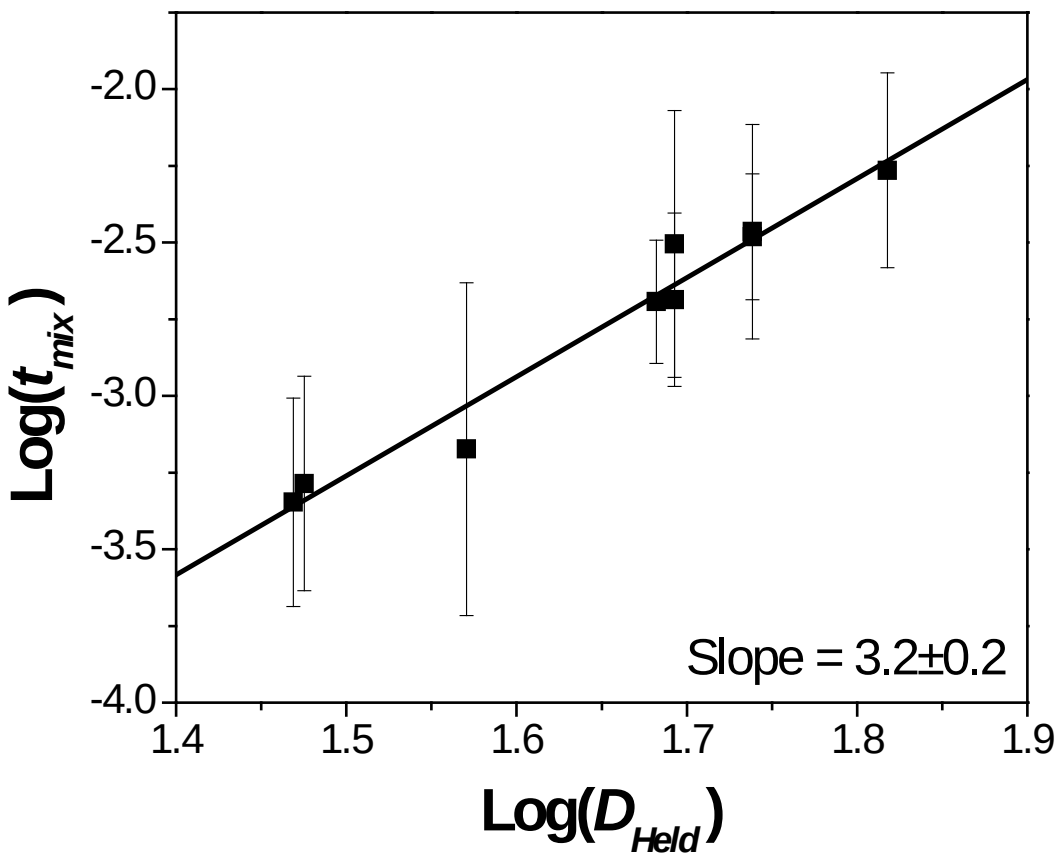

Figure S-4. A log-log plot of mixing time vs. held droplet diameter has a slope of ~3. This suggests that the mixing time is proportional to the volume of the held droplet.

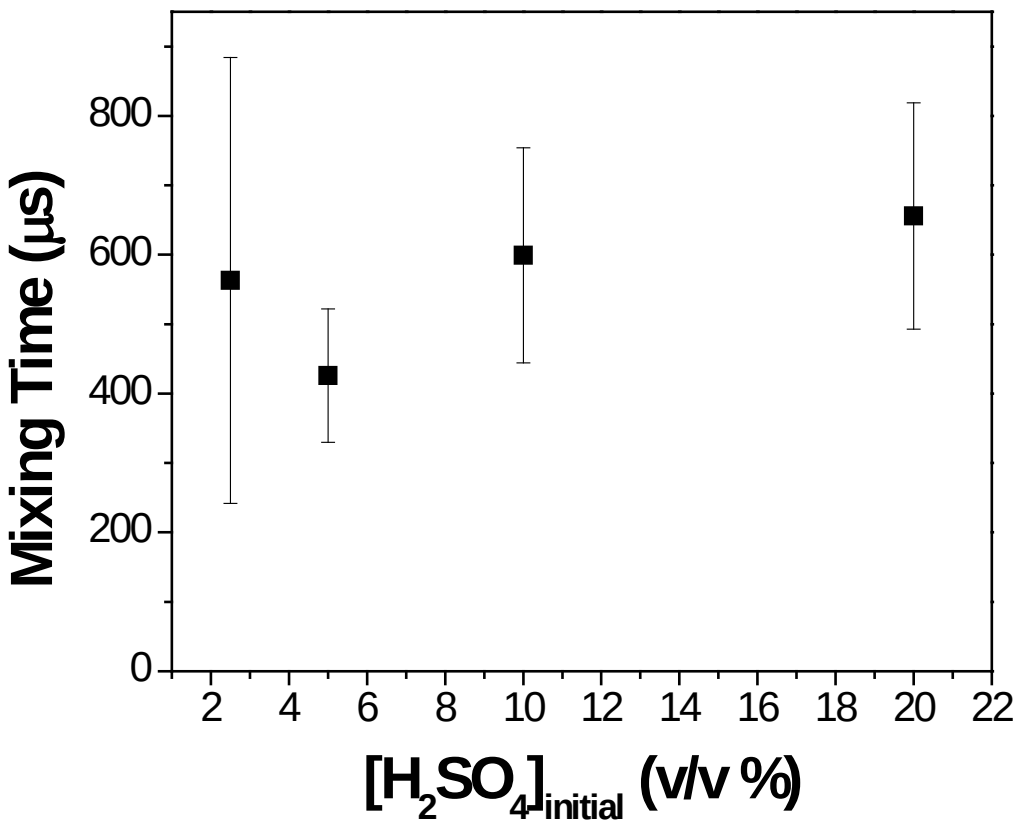

Figure S-5. Mixing times in the coalesced droplets are measured as a function of acid concentration in the merging droplet. The held RhB droplet had a constant diameter of 55±2 µm, and the merging sulfuric acid droplet had a constant diameter of 42±3 µs. The experimental mixing time is found to be invariable with concentration of acid.

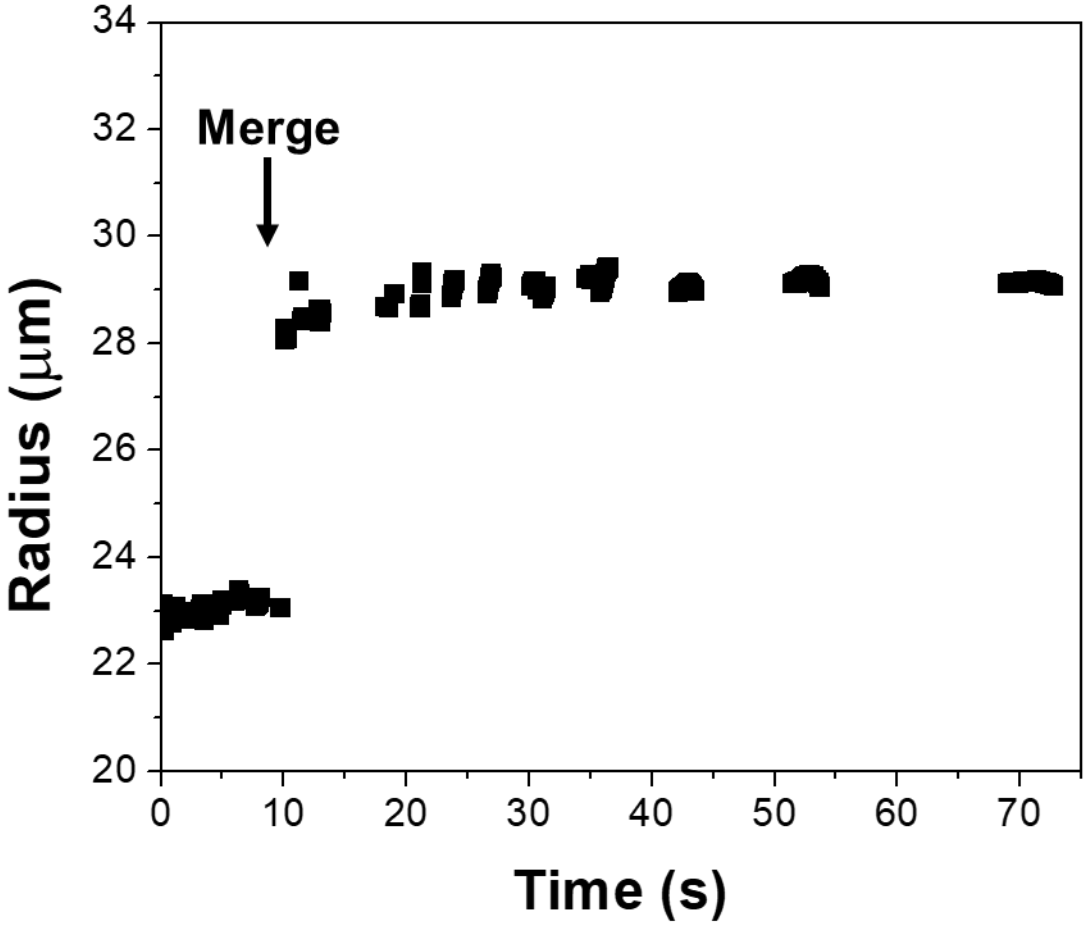

Figure S-6. An example of how the measured droplet radius changes over the course of a reaction. At t ≈ 10 s, the held and merging droplet coalesce which initiates the chemical reaction and increases the radius of the trapped droplet. The gaps in the measured radius are caused by poorly defined/separated Mie scattering fringes.

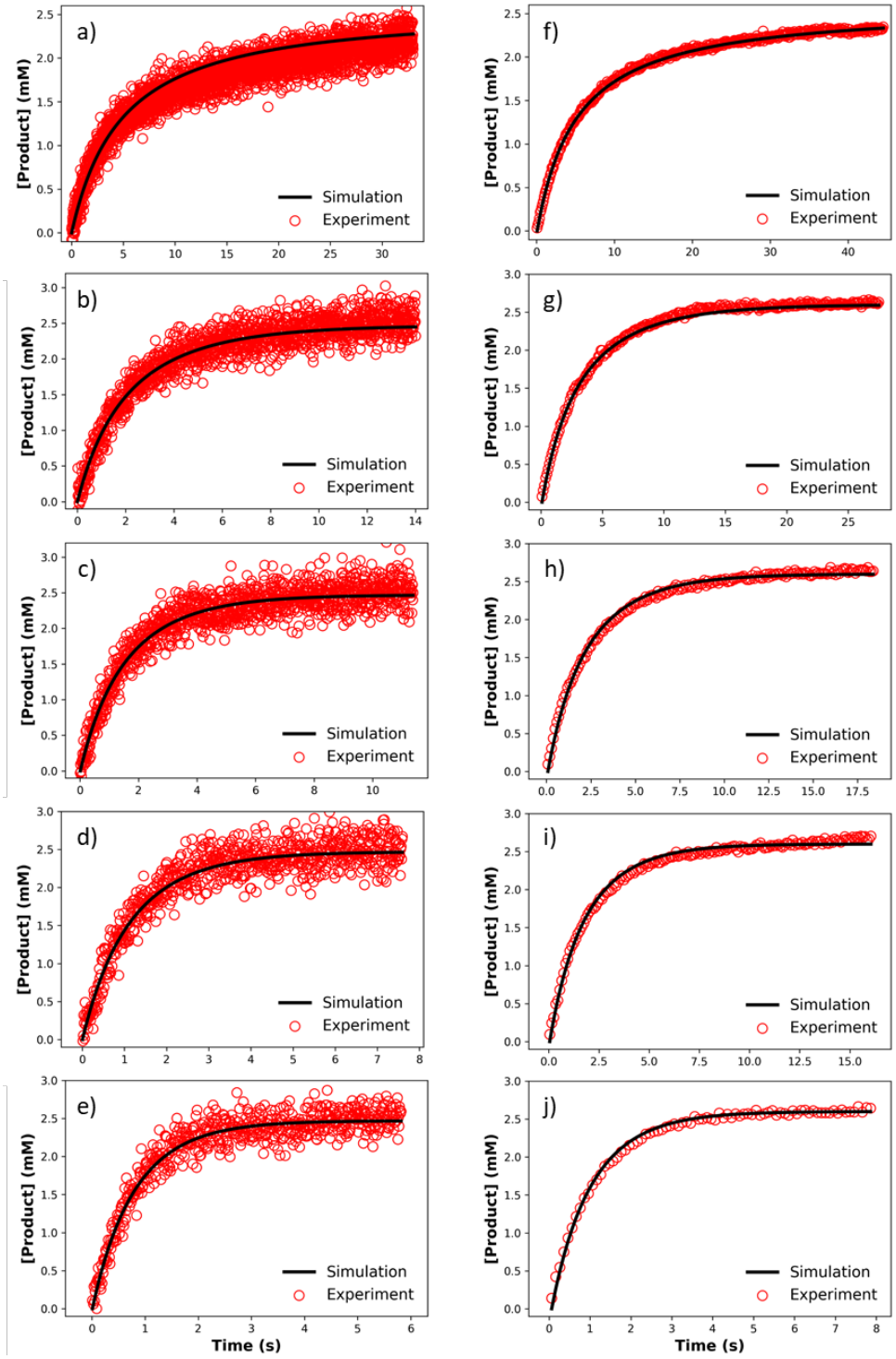

Figure S-7. Experimental and simulated product concentrations at different reaction conditions. a)-e) Correspond to reactions in droplets with 2.4±0.1 mM initial OPA concentration. The starting alanine concentrations are 2.8±0.1, 5.5 ±0.2, 8.1±0.4, 11.1±5, and 18±1 mM in panels a), b), c), d), and e), respectively. Panels f)-j) correspond to reactions in bulk with 2.6 mM initial OPA concentration. The starting alanine concentrations are 2.6, 5.2, 7.7, 10.4, and 16.7 mM in panels f), g), h), i), and j), respectively. Individual rate constants are tabulated in Table S-1.

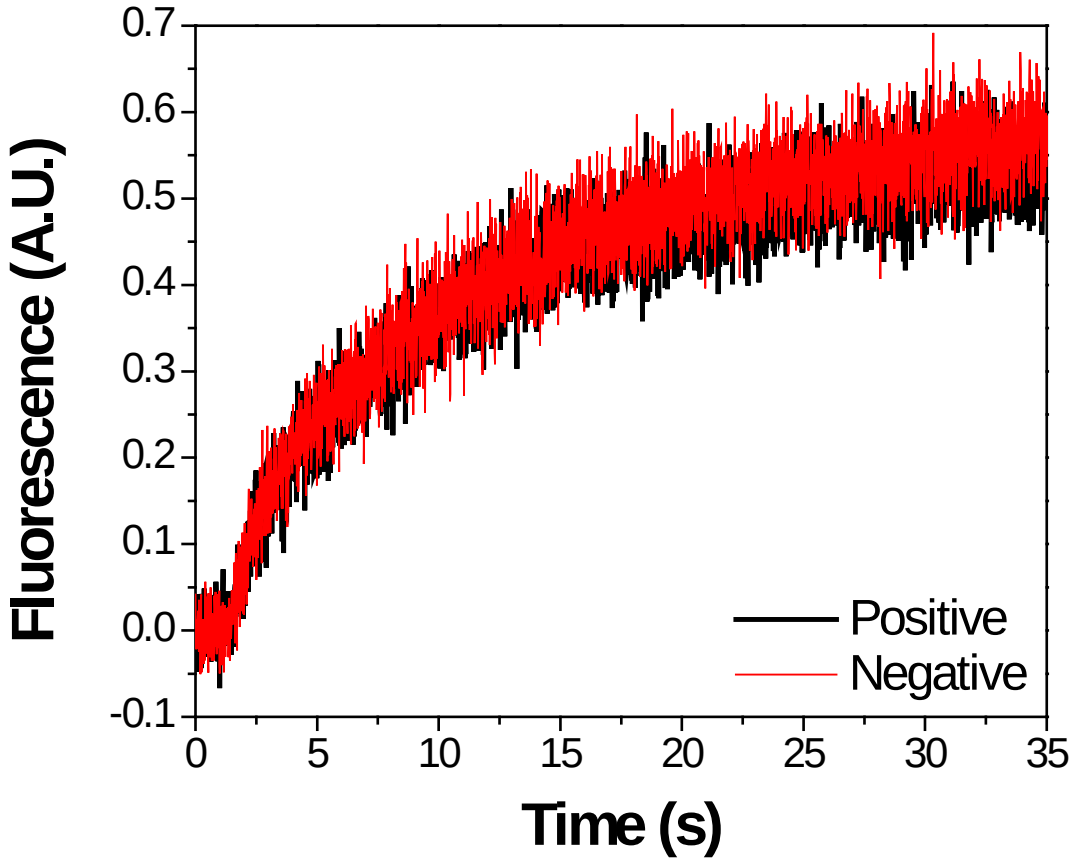

Figure S-8. The reaction of OPA and alanine in positively and negatively charged trapped droplets. Alanine and OPA both had initial concentrations of ~2.6 mM. Because the rate of reaction does not vary with the type of charge on the particle, the small amount of charge on the particle does not appear to influence the kinetics of the reaction.

Table S-1. Best fit rate constants in the bulk and droplet at different reaction conditions. At each condition, the initial concentration of OPA remains the same (2.6 mM in bulk and 2.4±0.1 mM in droplets). The approximate initial alanine concentrations are listed. The concentrations used for kinetic modelling are determined by the measured dilution factor (i.e. size of initial droplets).

~[Alanine] (mM)	**k_{bulk} (M^{-1} s^{-1})**	**$k_{droplet}$ (M^{-1} s^{-1})**
2.6	75.3	76.7
5.1	71.0	98.5
7.7	66.0	86.5
10.4	58.4	85.1
16.7	64.4	73.9
Average	67±6	84±10

Table S-2. Chemical structures of the ions detected in the single droplet PS mass spectrometry experiments.

Ion Detected	Chemical Structure	Molecular Weight (Da)
90 $[M+H]^+$	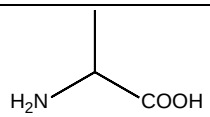	89
135 $[M+H]^+$ **157** $[M+Na]^+$	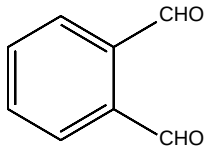	134
311 $[M+Na]^+$	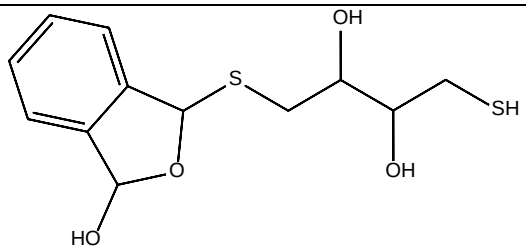	288
445 $[M+Na]^+$	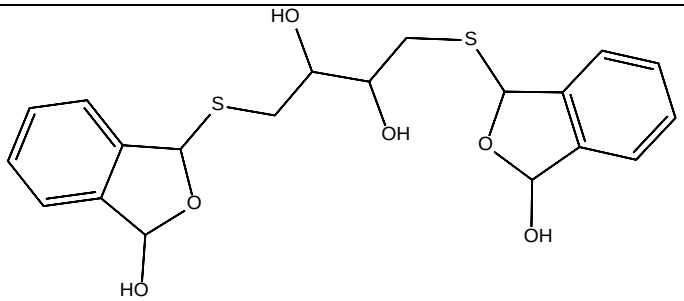	444
342 $[M+H]^+$	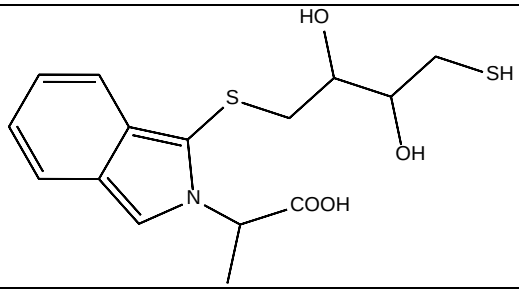	341
476 $[M+H]^+$	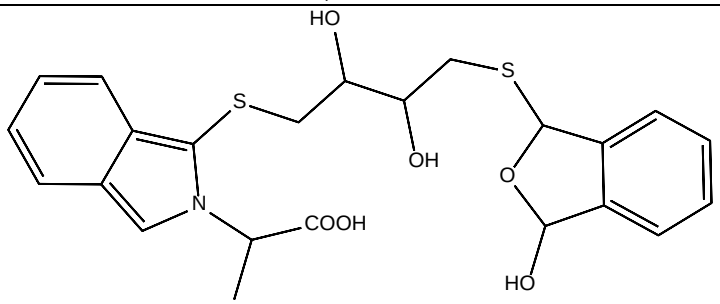	476